

Molecular Structure, Spectroscopy and Matrix Photochemistry of Fluorocarbonyl Iodide, FC(O)I

M. S. Chiappero,^[a] G. A. Argüello,*^[a] P. Garcia,^[b] H. Pernice,^[b] H. Willner,*^[b]
H. Oberhammer,^[c] K. A. Peterson,^[d] and J. S. Francisco^[e]

Abstract: The molecular structure of FC(O)I has been determined by gas electron diffraction. High-level ab initio methods, including coupled-cluster and the new correlation-consistent basis sets for fourth row elements, have been used to calculate the structure of FC(O)I. A comprehensive vibrational spectroscopic study (both IR and Raman) complemented by high-level calculations has also been performed. Furthermore, UV, mass, and NMR spectra have been recorded for

FC(O)I. The matrix photochemistry of FC(O)I has been studied with a low-pressure mercury lamp and with a high-pressure xenon lamp in combination with interference and cut-off filters. UV photolysis revealed the formation of the OC⋯IF and OC⋯FI com-

plexes and further photolysis of these complexes at $\lambda > 320$ nm resulted in a re-formation of FC(O)I. The structural conformation of the complexes has been characterized by comparing shifts in their CO and IF vibrational modes with respect to those of the free species. The structures, vibrational properties, and stability of the complexes were analyzed with the aid of coupled-cluster ab initio calculations.

Keywords: ab initio calculations • gas electron diffraction • matrix isolation • photochemistry • vibrational spectroscopy

Introduction

Structures, as well as spectroscopic and physical properties of the six possible carbonyl halides formed by F, Cl, and Br are well-known.^[1,2] Some of these compounds have also

been postulated as intermediates in atmospheric oxidation processes of halomethanes.^[3] As a consequence of the rising interest in such compounds, synthetic pathways and physical properties are known for most of them.^[1,2] In contrast, the knowledge about the four possible carbonyl iodides are minimal. The first iodinated carbonyl halide, FC(O)I, was prepared by Kwasnik almost 60 years ago.^[4,5] It was synthesized from IF₅ and 120 bar of CO in an autoclave according to Equation (1).



The determined physical properties (m.p. = -90°C, b.p. = 23.4°C, ρ_L (0°C) = 2.618 g mL⁻¹, ρ_L (16°C) = 2.470 g mL⁻¹, ρ_L (21.2°C) = 2.425 g mL⁻¹, and the interpolated vapor pressures for p_1 (-62°C) = 10 Torr, p_1 (-24°C) = 100 Torr are still the only ones known.

Herein, we suggest a modification of the above-mentioned synthetic path at atmospheric pressure and carry out a complete vibrational analysis as well as a gas electron diffraction (GED) study. NMR spectra have also been measured (¹⁹F, ¹³C, and ¹⁷O) and compared with those of other carbonyl halide fluorides. Another point of interest of the title compound is its role as an IF source. The latter was observed after the photolysis of FC(O)I in an argon matrix, which generated CO and IF in analogy to the photodecomposition of FC(O)H.^[6] It is well known that CO has the abil-

[a] Dr. M. S. Chiappero, Prof. Dr. G. A. Argüello
INFIQC (Departamento de Físico Química)
Facultad de Ciencias Químicas, Universidad Nacional de Córdoba
Ciudad Universitaria, 5000 Córdoba (Argentina)
E-mail: gaac@fisquim.fcq.unc.edu.ar

[b] Dipl.-Chem. P. Garcia, Dipl.-Chem. H. Pernice, Prof. Dr. H. Willner
Fakultät 4, Anorganische Chemie, Gerhard-Mercator-Universität
Duisburg
Lotharstrasse 1, 47048 Duisburg (Germany)
E-mail: willner@uni-wuppertal.de

[c] Prof. Dr. H. Oberhammer
Institut für Physikalische und Theoretische Chemie, Universität Tübingen
72076 Tübingen (Germany)
E-mail: heinz.oberhammer@uni-tuebingen.de

[d] Prof. Dr. K. A. Peterson
Department of Chemistry, Washington State University
Pullman, WA 99164-4630 (USA)

[e] Prof. Dr. J. S. Francisco
Department of Chemistry, Purdue University
West Lafayette, IN 47907 (USA)

[*] Present address: FB 9, Anorganische Chemie, Bergische Universität Wuppertal, Gaußstrasse 20, 42097 Wuppertal (Germany)

ity to form weakly bonded complexes. The origin of this phenomenon is the capability of CO to act as a weak σ -Lewis base as well as a weak π -Lewis acid.^[7,8] In recent years, there have been many reports dealing with the interaction of CO with halogens and interhalogens in the gas phase that used matrix isolation techniques.^[9–15] To support the interpretation of all experimental results, high-level ab initio calculations have been carried out.

Results and Discussion

It was found that FC(O)I was formed by passing CO at atmospheric pressure over a heated mixture of IF₅ and I₂. We assume that IF₅ and I₂ form IF molecules in an equilibrium which react in turn with CO according to Equations (2) and (3).



The reaction enthalpy for Equation (3) amounts to 27 kcal mol⁻¹ exothermic according to the ab initio calculations (see below).

Structure of FC(O)I: *Gas electron diffraction results:* The experimental radial distribution function (RDF), which was derived by Fourier transformation of the modified molecular intensities, is shown in Figure 1. The modified molecular in-

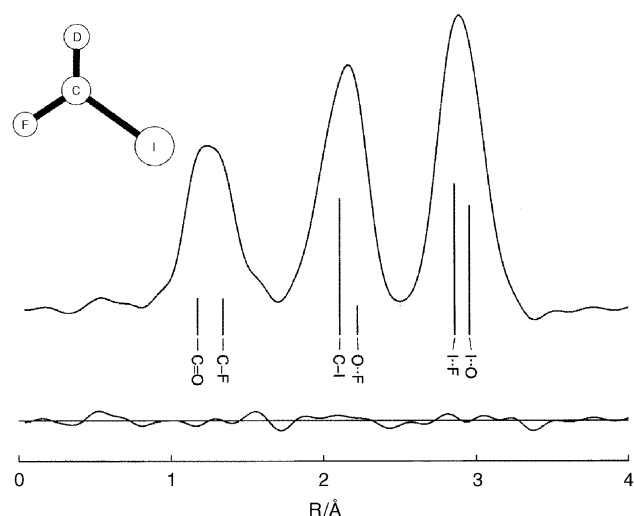


Figure 1. Experimental radial distribution function and difference curve. Positions of interatomic distances are indicated by vertical bars.

tensity ($M(s) = I(\text{molecular})/I(\text{atomic})$) of FC(O)I is very weak because of the high atomic intensity $I(\text{atomic})$ and the large phase shift (imaginary part of scattering amplitude) of iodine, owing to which the contributions of the bonded C–I and nonbonded I... (O, F) distances to the molecular intensities $I(\text{molecular})$ vanish near $s = 20 \text{ \AA}^{-1}$. Therefore, the relative noise level in the intensities is higher than usual, leading to larger residuals in the RDF. A molecular model de-

rived from the RDF was refined by least-squares fitting of the modified molecular intensities. Assuming planarity of FC(O)I, five geometric parameters ($p1$ to $p5$) and five vibrational amplitudes ($L1$ to $L6$ or $L5$, respectively) were refined simultaneously in the analysis. The amplitude for the O...F distance in FC(O)I was constrained to the calculated value. The following correlation coefficient had a value larger than $|0.6|$ and $p5L5 = -0.91$. The final results for the geometric parameters are listed in Table 1. Averaged

Table 1. Relevant geometric parameters of carbonyl fluorides FC(O)X.

	C=O	C–F	C–X	O=C–F	F–C–X
FC(O)F ^[a]	1.1717(13)	1.3157(8)	1.3157(8)	126.15(8)	107.70(12)
FC(O)Cl ^[b]	1.173(2)	1.334(2)	1.725(2)	123.7(2)	108.8(3)
FC(O)Br ^[c]	1.174(6)	1.326(7)	1.896(4)	122.3(7)	109.7(13)
FC(O)I ^[d]	1.177(7)	1.343(8)	2.109(7)	123.8(13)	111.1(21)
FC(O)H ^[e]	1.188(4)	1.346(3)	1.108(11)	122.3(2)	108(4)

[a] r_z structure from reference [16]. [b] r_z structure from reference [17]. [c] r_a structure, G.A. Argüello, H. Willner, H. Oberhammer, unpublished. [d] r_a structure, this work. [e] r_g structure from reference [18].

modified molecular intensities in the ranges 2–18 and 18–35 \AA^{-1} in intervals of $\Delta s = 0.2 \text{ \AA}^{-1}$ ($s = (4\pi/\lambda) \sin \theta/2$, $\lambda =$ electron wavelength, $\theta =$ scattering angle) are shown in Figure 2.

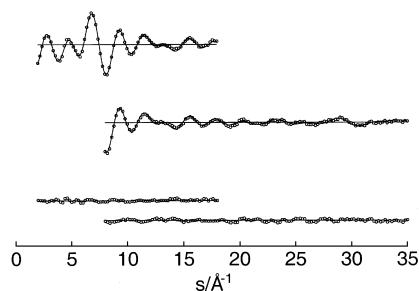


Figure 2. Averaged modified molecular intensities for long (above) and short (below) nozzle-to-plate distances and residuals.

The geometric parameters of the FC(O) group in carbonyl fluorides FC(O)X are summarized in Table 1. Although experimental errors conceal clear trends for some parameters, a general lengthening of the C=O and C–F bond lengths with decreasing electronegativity of X can be observed and the F–C–X angle increases in this series.

Ab initio calculated structure: The equilibrium geometry for FC(O)I was calculated at the CCSD(T) level of theory with three basis sets: aug-cc-pVDZ, aug-cc-pVTZ, and aug-cc-pVQZ (see Table 2). The calculations show that the size of the basis set is very important for the accurate prediction of the FC(O)I structure. For a comparison between experimental and calculated bond lengths, the systematic differences between r_a values from experiment and equilibrium r_e distances from calculations have to be considered. r_a bond lengths are estimated to be 0.002 to 0.005 \AA longer than r_e values. At the CCSD(T)/aug-cc-pVDZ level of theory, all

Table 2. Experimental and calculated structure for FC(O)I.

Coordinate ^[a]	CCSD(T)			Expt. GED (r_a) ^[b]
	aug-cc-pVDZ	aug-cc-pVTZ	aug-cc-pVQZ	
$r(\text{C}=\text{O})$	1.189	1.180	1.176	1.177(7)
$r(\text{C}-\text{F})$	1.363	1.338	1.334	1.343(8)
$r(\text{C}-\text{I})$	2.129	2.117	2.113	2.109(7)
$\theta(\text{FC}=\text{O})$	123.1	123.3	123.4	123.8(14)
$\theta(\text{IC}=\text{O})$	127.1	126.7	126.7	125.1(16)
$\theta(\text{FCI})$	109.8	110.0	110.0	111.1(21)

[a] r in Å, θ in °. [b] Error limit is 3σ values.

bond lengths are overestimated compared to experimental ones. The C–F and C–I bonds are also overestimated by 0.020 Å. Inclusions of f -polarization functions (i.e., VTZ and larger) are, at a minimum, the smallest size of basis set that could be used to reasonably predict the structure of FC(O)I compared to experiment. The rms error for the bonds in FC(O)I with the aug-cc-pVDZ basis set is 0.022 Å while for the aug-cc-pVTZ basis set it is 0.007 Å. At the CCSD(T)/aug-cc-pVQZ level of theory, the FC(O)I structure falls within the experimental uncertainty of the structure derived from the GED study. We should comment that our preliminary studies of FC(O)I with LANL2DZ effective core potentials and basis sets did not produce results that were reliable with the CCSD(T) method. This suggested that these basis sets were much too small.

Vibrational spectroscopy: IR and Raman results: FC(O)I is a planar tetra-atomic asymmetric rotator with C_s symmetry and the six vibrational modes in the symmetry classes $5A' + 1A''$ are all expected to be IR- and Raman-active. The vibration of type A'' is antisymmetric with respect to the symmetry plane in direction of I_c and therefore for δ_{oop} a band contour of the type “C” with a strong Q branch is expected. The only absorption band that presents such a characteristic is found at 567 cm^{-1} (ν_6 , Figure 3). The five A' modes are of hybrid “A/B” character because here the dipole moment changes are not parallel to I_a or I_b . Furthermore, from characteristic wavenumbers, the carbonyl stretching is expected to be at about 1900 cm^{-1} ($\nu_1 = 1848\text{ cm}^{-1}$) and the C–F

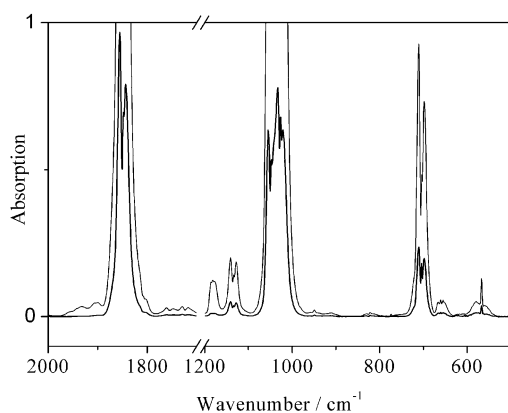


Figure 3. IR spectrum of gaseous FC(O)I at 25°C, with an optical path length of 19.5 cm and a pressure of 5 mbar (upper trace) and 1 mbar (lower trace)

stretching at around 1100 cm^{-1} ($\nu_2 = 1027\text{ cm}^{-1}$). The latter is greatly disturbed by an anharmonic resonance with the combination band at 1048 cm^{-1} .

Because of the large polarizability of iodine, $\nu(\text{C}-\text{I})$ will result in a strong Raman line. This band can be seen in the Raman spectrum at 346 cm^{-1} (ν_4 , Figure 4). The remaining

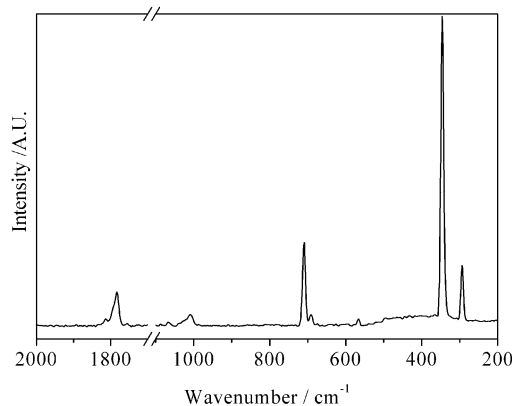


Figure 4. Raman spectrum of a solid sample of FC(O)I measured at -196°C with a resolution of 4 cm^{-1} .

fundamental modes ($\nu_3 = 704\text{ cm}^{-1}$, $\delta(\text{FCO})$; $\nu_5 = 294\text{ cm}^{-1}$, $\rho(\text{FCO})$) were assigned on the basis of the calculated band positions and displacement vectors. Only four of the six fundamentals were visible in the gas-phase IR spectrum in the range $4000\text{--}400\text{ cm}^{-1}$ along with some overtones and combinations.

Matrix-isolation techniques enable the measurement of IR spectra without rotational structure. Therefore, it facilitates the assignment of normal modes, their isotopic satellites, and combinations. All vibrational data are listed in Table 3.

Ab initio-calculated vibrational wavenumbers: The fundamental harmonic vibrational frequencies for FC(O)I were also calculated with CCSD(T)/aug-cc-pVDZ and CCSD(T)/aug-cc-pVTZ levels of theory. The calculations confirm the vibrational mode assignments. We also find that the better agreement with experimental vibrational wavenumbers comes from those calculated at the CCSD(T)/aug-cc-pVTZ level of theory. The rms error is 20.5 cm^{-1} for the CCSD(T)/aug-cc-pVDZ method and 16.8 cm^{-1} for the CCSD(T)/aug-cc-pVTZ method as compared to the experimental gas-phase IR wavenumbers (Table 3). This trend of improved results with increased basis set, particularly with the basis set augmented with f -polarization functions, is consistent with that observed for the geometry calculations. In addition, the largest deviations with the aug-cc-pVTZ basis set occur for the C=O and C–F stretching vibrations, which can largely be attributed to the effects of anharmonicity.

UV spectroscopy: The gas-phase UV/Vis spectrum of FC(O)I exhibits two absorption bands at $\nu = 207$ and 255 nm (Figure 5). The highest energy band could correspond to an allowed $\pi\text{--}\pi^*$ transition and the band at 255 nm

Table 3. Observed and calculated IR and Raman wavenumbers for FC(O)I.

gas phase	IR		Raman solid, -196 °C	Calculated ^[b]		Assignment	Approx. description of mode
	Ar matrix	I ^[a]		aug-cc-pVDZ	aug-cc-pVTZ		
2066 1848	2056.9	1.9	1778 (m)	1846	1872	2 ($\nu_3 + \nu_4$)	$\nu(\text{C}=\text{O})$
	2032.4	2.8				$2\nu_2$	
	1836.6	100				A', ν_1	
	1794.3	1.5				^{13}C	
	1753.8	0.65				$2\nu_3 + \nu_4$	
1134	1716.3	1.1	1008 ^[c] (m)	1006	1061	$\nu_2 + \nu_3$	$\nu(\text{CF})$
	1133.2	5.3				$2\nu_3$	
	1048	26				$\nu_3 + \nu_4$	
1027 ^[c]	1020.6 ^[c]	96	711 (s)	679	705	A', ν_2	$\delta(\text{FCO})$
	998.2	0.70				^{13}C	
704	704.6	19	567 (w)	554	571	A', ν_3	δ oop
	589.6	0.44				346 (vs)	
567	566.2	5.8	294 (m)	286	291	A', ν_5	$\delta(\text{FCO})$

[a] Relative integrated intensities. [b] CCSD(T). [c] Disturbed by anharmonic resonance with ($\nu_3 + \nu_4$), see text.

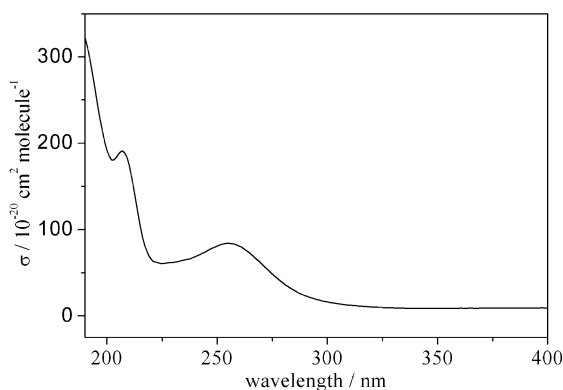


Figure 5. UV spectrum of FCOI in the gas phase.

to the forbidden $n-\pi^*$ transition. Both are characteristic for the presence of a $\text{C}=\text{O}$ group in the molecule. The absence of a vibrational structure is evident in the spectrum as is the case for $\text{ClC}(\text{O})\text{Cl}$ and $\text{FC}(\text{O})\text{Cl}$.^[19,20] The experimental cross-sections are relatively high in the UV region and extremely low in the visible region (the neat compound is colorless).

NMR spectroscopy: All NMR data are presented in Table 4 and are compared to those for the other members of the series $\text{FC}(\text{O})\text{X}$ ($\text{X} = \text{F}, \text{Cl}, \text{Br}$).^[2] There is a clear trend in all magnitudes going from fluoride to iodide. In the series of compounds $\text{FC}(\text{O})\text{X}$, $\delta(^{19}\text{F})$ and $\delta(^{17}\text{O})$ increase to higher

Table 4. NMR data of $\text{FC}(\text{O})\text{I}$ and related compounds.

Compound	$\delta(^{19}\text{F})$	$\delta(^{13}\text{C})$	$\delta(^{17}\text{O})$ ^[a]	$^1J(\text{C},\text{F})$ [Hz]	$^2J(\text{O},\text{F})$ [Hz]	Ref.
$\text{FC}(\text{O})\text{I}$ ^[b]	121.2	98.1	435.7	445.8	49.5	^[c]
$\text{FC}(\text{O})\text{Br}$	84.7	127.6	401.9	404.2	41.7	^[d]
$\text{FC}(\text{O})\text{Cl}$	60.0	139.9	375.1	366.4	37.4	^[d]
$\text{FC}(\text{O})\text{F}$	-20.4	134.1	259.5	310.3	37.6	^[d]

[a] Measured with respect to external H_2O . [b] All spectra were measured on the same sample at -40°C with CD_2Cl_2 as the solvent (1:1) and traces of CFCl_3 as internal standards. [c] This work. [d] Reference [12].

resonance frequencies with decreasing electronegativity of the halogen X. This indicates that the contribution of the paramagnetic term to the chemical shift is greater than the diamagnetic electron-withdrawing effect.

In the case of the $\delta(^{13}\text{C})$ chemical shifts, the σ and π effect are working against each other causing a maximum shift for $\text{FC}(\text{O})\text{Cl}$. The $^1J(\text{C},\text{F})$ coupling constants increase with increasing $\pi(\text{C}-\text{F})$ bond strength and $\text{FC}(\text{O})\text{I}$ with the largest $^1J(\text{C},\text{F})$ coupling constant should show the strongest $\pi(\text{C}-\text{F})$ bond contribution.

Mass spectrometry: The mass spectrum of $\text{FC}(\text{O})\text{I}$ at 70 eV, shows the following fragment ions, m/z (% ion): 174 (100, $[\text{FC}(\text{O})\text{I}]^+$), 155 (3, $[\text{IC}(\text{O})]^+$), 146 (1, $[\text{IF}]^+$), 127 (44, $[\text{I}]^+$), 47 (23, $[\text{FC}(\text{O})]^+$), 31 (3, $[\text{CF}]^+$). We could not observe ionic fragments $m/z < 30$; however, the features in the mass spectrum are undoubtedly caused by $\text{FC}(\text{O})\text{I}$. The highest peak corresponds to the molecular ion and the two triatomic resonance-stabilized fragment ions $[\text{IC}(\text{O})]^+$ and $[\text{FC}(\text{O})]^+$ are present.

Matrix photochemistry of $\text{FC}(\text{O})\text{I}$: Photoisomerization of matrix-isolated $\text{FC}(\text{O})\text{I}$: Complexes between CO and halogens or interhalogens have been extensively studied in recent years both theoretically and experimentally in the gas phase as well as isolated in noble gas matrices.^[9,14,15,21,22] To our knowledge, no CO/IF complex has been reported so far. The high instability of IF does not allow its handling in the gas phase and therefore co-deposition of CO and IF in a matrix has not been possible. Here we overcome this problem by in-situ generation of CO/IF complexes in a matrix. By adopting the same procedure as in the UV photolysis of formyl fluoride, which resulted in CO/HF complexes in high yields,^[6] we could directly observe the formation of CO/IF from photolysis of $\text{FC}(\text{O})\text{I}$ isolated in argon matrices. There are four possible connectivities between CO and IF: $\text{OC}\cdots\text{IF}$ (1), $\text{OC}\cdots\text{FI}$ (2), $\text{CO}\cdots\text{IF}$ (3), $\text{CO}\cdots\text{FI}$ (4). According to the literature, complexes formed as a result of a charge transfer from the carbon atom are more stable than those which involve the oxygen atom. In that case, because of the C–O bond polarization, a blue shift with respect to free CO and a red shift with respect to the free IF absorption is expected.^[23] Ab initio calculations have shown that those complexes in which the more polarizable halogen accepts the charge are energetically favored and that a part of this charge is further transferred to the other halogen atom.

The complex $\text{OC}\rightarrow\text{BrCl}$ shows a shift of $+9.4\text{ cm}^{-1}$ in the CO absorption while the opposite is shown by the complex $\text{OC}\rightarrow\text{ClBr}$ which amounts to -0.5 cm^{-1} ,^[9] thus we expect the stability of the series to be: **1 > 2 > 3 > 4**.

Difference IR spectra of FC(O)I before and after UV photolysis are depicted in Figure 6. Photolysis with a Xe arc lamp in combination with a 254 nm interference filter (upper trace) produces negative bands from the photolyzed FC(O)I (1836.6 cm⁻¹, 1020.6 cm⁻¹, 704.6 cm⁻¹, and 566.2 cm⁻¹) and simultaneously raising (positive) peaks grow

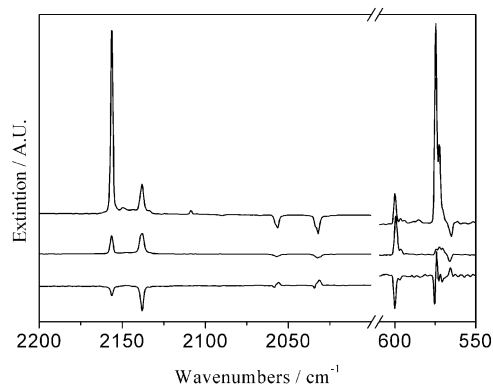


Figure 6. Difference matrix IR spectra of FC(O)I photolysis (before minus after). Upper trace: 60 min photolysis with a Xe arc lamp (150 W) and an interference filter ($\lambda = 254$ nm). Bands of the CO/IF complexes are pointing upwards and those of FC(O)I are pointing downwards. Middle trace: Photolysis of FC(O)I with the unfiltered light of a low-pressure mercury lamp (35 W) for 60 min ($\lambda < 254$ nm). Lower trace: photolysis of the CO/IF complexes with a Xe arc lamp with a cut-off filter ($\lambda = 320$ nm).

at 2156.3 cm⁻¹, 2138.2 cm⁻¹, 600.1 cm⁻¹, and 574.8 cm⁻¹ (Figure 6 upper trace). The new features were assigned to the formation of CO/IF complexes. The absorption bands at 574.8 cm⁻¹ and 600.1 cm⁻¹ were assigned to the IF stretching mode of OC \cdots IF and OC \cdots FI, respectively, both red-shifted with respect to IF isolated in an argon matrix (603 cm⁻¹). Matrix-isolated IF was produced by heating a I₂/F₂ mixture at 400 °C, highly diluted in argon, in the spray-on nozzle of the matrix-isolation device. In the gas phase, IF was observed at 610.258 cm⁻¹.^[24]

The band at 2156.3 cm⁻¹ can be assigned to the blue-shifted CO stretching mode of the OC \cdots IF complex (for OC \cdots BrCl 2147.9 cm⁻¹).^[9] The feature at 2138.2 cm⁻¹, which on the first sight appeared to be free CO in argon matrix (2138.3 cm⁻¹),^[6] can be unambiguously assigned to OC \cdots FI (for OC \cdots ClBr 2138.0 cm⁻¹),^[9] with the help of quantum-chemical calculations and further photolysis experiments.

Besides some small peaks assigned to FC(O)F (1937.6 and 1909.5 cm⁻¹), no further bands were found in the proximity of 2000 cm⁻¹ that could indicate the presence of other complexes, which should show a red shift with respect to the free CO.

Photolysis of FC(O)I with unfiltered light from a low-pressure mercury lamp yielded product bands with clearly different relative band intensities (Figure 6, middle trace). For this photolysis we found a higher amount of the less stable OC \cdots FI complex. Finally, we were able to observe the disappearance of both CO/IF complexes and re-formation of FC(O)I after photolysis at $\lambda = 320$ nm (Figure 6, lower trace), and it is interesting to note that the photolysis rate of

OC \cdots FI is higher than that of the OC \cdots IF complex. Obviously, the long wavelength absorber is IF. During photolysis of the IF molecule in the matrix cage it dissociates into F and I atoms. In the case of the OC \cdots FI photolysis, FC(O)I is immediately reformed via the COF radical. In the case of OC \cdots IF, the F atom must migrate before it can attack the CO molecule.

All experimental and calculated wavenumbers and shifts of the CO/IF complexes are listed in Table 5.

Table 5. Calculated and observed fundamental vibrational wavenumbers and wavenumber shifts for CO/IF complexes.

Species	Mode number	CCSD(T)		Wavenumber shift ^[a,b]	
		aug-cc-pVDZ	aug-cc-pVTZ	$\Delta\nu(\text{CO})$	$\Delta\nu(\text{IF})$
OC-FI	1 (Σ)	2105	2144 (2138.2) ^[c]	0 (-0.1)	
	2 (Σ)	609	615 (600.1)		-2 (-3)
	3 (Π)	101	100		
	4 (Σ)	42	43		
	5 (Π)	39	37		
	6 (Π)	30	29		
OC-IF	1 (Σ)	2132	2166 (2156.3)	+22 (+18)	
	2 (Σ)	584	585 (574.8)		-32 (-28)
	3 (Π)	251	278		
	4 (Σ)	93	106		
	5 (Π)	73	77		
CO-IF	1 (Σ)	2093	2131	-13	
	2 (Σ)	608	615		-2
	3 (Π)	85	89		
	4 (Σ)	72	75		
	5 (Π)	38	39		

[a] $\Delta\nu(\text{CO}) = \nu(\text{CO})_{\text{complex}} - \nu(\text{CO})_{\text{free}}$; $\Delta\nu(\text{IF}) = \nu(\text{IF})_{\text{complex}} - \nu(\text{IF})_{\text{free}}$.
 [b] Calculated at the CCSD(T)/aug-cc-pVTZ level of theory. [c] Values in parenthesis are the experimental data

The thermal stability of FC(O)I was studied in a separate experiment. Heating of the spray-on nozzle to 400 °C caused no change in the resulting IR matrix spectra. Hence the molecule is resistant against C–I bond fission and its thermal instability in the condensed phase may be attributed to bimolecular (or heterogeneous) reactions.

Ab initio calculations of the structure and spectroscopy of CO/IF complexes: As mentioned in the previous section, there are four connectivities between CO and IF: OC \cdots IF (**1**), OC \cdots FI (**2**), CO \cdots IF (**3**), CO \cdots FI (**4**). We performed preliminary optimizations with the LANL2DZ effective core basis set with the B3LYP, MP2, QCISD, and CCSD(T) methods. Minimum energy structures were only obtained for the first three connectivities (Table 6). We were not successful in finding a stable minimum for the CO \cdots FI configuration. It was verified that the minima found for the OC \cdots IF, OC \cdots FI, and CO \cdots IF complexes were indeed true minima by vibrational frequency calculations in which no imaginary frequencies were obtained. The relative stability of FC(O)I in comparison with the complexes is also presented in Table 6. The preliminary structures of the complexes were

Table 6. Total energies, relative stability, and bond energies for FC(O)I complexes.

CCSD(T)	Species				FC(O)I
	OC-FI	OC-IF	CO-IF		
Total energies (Hartree)					
aug-cc-pVDZ	-509.4737622	-509.4819852	-509.4755469		-509.50912
aug-cc-pVTZ	-509.6959032	-509.7053999	-509.6978851		-509.73796
aug-cc-pVQZ	-509.7687047	-509.7782012	-509.7705940		-509.81060
relative stability [kcal mol ⁻¹]					
aug-cc-pVDZ	5.16	0.0	4.04		
aug-cc-pVTZ	5.96	0.0	4.71		
aug-cc-pVQZ	5.96	0.0	4.78		
bond energies, D_e [kcal mol ⁻¹]					
aug-cc-pVDZ	1.26	6.42	2.38		
aug-cc-pVTZ	1.12	7.08	2.37		
aug-cc-pVQZ	1.03	6.99	2.21		
stability relative to FC(O)I [kcal mol ⁻¹]					
aug-cc-pVDZ	22.1	17.0	21.1		
aug-cc-pVTZ	26.4	20.4	25.1		
aug-cc-pVQZ	26.3	20.3	25.1		

then used as initial starting structures for the CCSD(T) geometry optimizations with correlation-consistent basis sets. The optimized geometries for the three complexes are given in Table 7. It is unexpected that the complex OC...FI shows an OCF angle close to 102°. Calculated geometry differences in the C–O and I–F bonds as a result of complexation are given in Table 8. It is interesting to note that the largest structural shift in the three complexes comes from the OC...IF complex, particularly in the I–F bond. All the calculations (CCSD(T)/aug-cc-pVDZ, CCSD(T)/aug-cc-pVTZ, and CCSD(T)/aug-cc-pVQZ methods) predicted a geometry shift of $\approx +0.024 \pm 0.001$ Å in the I–F bond length. The

Table 7. Calculated equilibrium geometries for OC-FI, OC-IF, and CO-IF complexes.

Species	CCSD(T)	Coordinates				$\theta(XYZ)^{[a]}$
		$r(\text{CO})$	$r(\text{CF})$	$r(\text{IF})$	$r(\text{CI})$	
OC-FI	aug-cc-pVDZ	1.147	3.030	1.955		102.5
	aug-cc-pVTZ	1.136	3.013	1.929		102.1
	aug-cc-pVQZ	1.132	3.037	1.917		101.3
OC-IF	aug-cc-pVDZ	1.143		1.974	2.648	180
	aug-cc-pVTZ	1.132		1.950	2.556	180
	aug-cc-pVQZ	1.128		1.941	2.545	180
CO-IF	aug-cc-pVDZ	1.149		1.956		3.047
	aug-cc-pVTZ	1.138		1.929		3.019
	aug-cc-pVQZ	1.133		1.918		3.007

[a] X = O or C, Y = C or O, Z = F or I.

Table 8. Calculated geometry differences^[a] for the different complexes as well as for free CO and IF.

Molecular complex	CCSD(T)	$\Delta r(\text{CO})$	$\Delta r(\text{IF})$
OC-FI	aug-cc-pVDZ	0.000	+0.001
	aug-cc-pVTZ	0.000	+0.002
	aug-cc-pVQZ	0.000	+0.001
OC-IF	aug-cc-pVDZ	-0.004	+0.020
	aug-cc-pVTZ	-0.004	+0.023
	aug-cc-pVQZ	-0.004	+0.025
CO-IF	aug-cc-pVDZ	+0.002	+0.002
	aug-cc-pVTZ	+0.002	+0.002
	aug-cc-pVQZ	+0.001	+0.002

[a] $\Delta r(\text{CO}) = r(\text{CO})_{\text{complex}} - r(\text{CO})_{\text{free}}$, $\Delta r(\text{IF}) = r(\text{IF})_{\text{complex}} - r(\text{IF})_{\text{free}}$.

next shift is in the C–O bond where theory consistently shows a shortening of the C–O bond by 0.004 Å. These are significant geometry shifts when compared to shifts for the OC...FI and CO...IF complexes, where the structural interactions are less. The structure that shows the largest interaction, as shown in Table 6, is the structure that is most stable. This is also consistent with observations in the literature for complexes of CO with BrCl.^[9] We estimated that the binding energy in OC...IF is ≈ 7 kcal mol⁻¹ at the CCSD(T)/aug-cc-pVQZ level of theory. This is

the strongest binding of the three complexes; the values of other structures lie between 1 and 2 kcal mol⁻¹. Because there is a large shift in the bonds of the CO and IF molecules in the OC...IF complex, these structural changes should produce significant shifts in the vibrational spectrum. The fundamental vibrational frequencies for the complexes are listed in Table 5. The geometry change in the C–O bond is for the bond to contract. A shorter C–O bond should result in a shift to a higher frequency. Indeed, the calculations at the CCSD(T)/aug-cc-pVTZ level of theory show a shift to higher wavenumbers of 22 cm⁻¹. Experiments show this shift to be 18 cm⁻¹, which is in excellent agreement with

the calculations. The largest geometry change is in the I–F bond, where the I–F bond is elongated by 0.024 ± 0.001 Å in the complex, suggesting a weakening of this bond. The CCSD(T)/aug-cc-pVTZ vibrational frequencies and shift show that the I–F bond is lower in frequency and is shifted to a lower wavenumber by 32 cm⁻¹. The red shift in the experiment is observed to be 28 cm⁻¹, which is also in excellent agreement with the calculations.

Experimental Section and Computational Methods

Caution: As for other carbonyl halides, FC(O)I must be considered to be a toxic gas.

Apparatus: Volatile materials were manipulated in a glass vacuum line equipped with two capacity pressure gauges (221 AHS-1000 and 221 AHS-100, MKS Baratron (USA)), three U-traps and valves with PTFE stems (Young (UK)). The vacuum line was connected to an IR gas cell (optical path length 200 mm, Si wafer windows, 0.6 mm thick) contained in the sample compartment of the FTIR instrument (Nicolet Impact 400D). This arrangement made it possible to follow the course of reactions and the purification process of the products. The products were

stored in flame-sealed glass ampoules in liquid nitrogen. The ampoules were opened at the vacuum line by means of an ampoule key,^[25] and appropriate amounts were taken out and before the ampoules were flame-sealed again.

Synthesis of FC(O)I: The synthesis was carried out in a train of three traps connected with standard connectors and joints and provided with glass valves with PTFE stems (Young, (UK)). A slow flow of CO gas was passed through a U-trap containing a mixture of IF₃:2I₂ at 90 °C. Downstream, two cold traps were used to collect the volatile products. In the first one, at –30 °C, the iodine and IF₃ were retained, and in the second one, kept at –183 °C, the FC(O)I was trapped together with F₂C(O), CO₂, and SiF₄. The raw product was purified by trap-to-trap condensations through three U-traps held at –90 °C, –120 °C, and –196 °C, respectively. In addition to molecular iodine (not detected in the IR spectra), other compounds found during the purification process were COF₂, CO₂, and SiF₄, which had been produced by the title compound reacting with H₂O on the glass walls. All of them were identified by their known IR spectra and discarded. The distillation was repeated several times, and the content of the trap at –120 °C was collected in a storage vessel held at –196 °C. Subsequently, 2 g of FC(O)I with traces of iodine were obtained (about 5% yield related to CO). Further attempts at purification were unsuccessful since the product reacted with the glass walls to produce more I₂, COF₂, SiF₄, and CO₂. In addition, the purity of the sample was checked by ¹⁹F, ¹³C, and ¹⁷O NMR measurements (>98%).

Gas electron diffraction: Electron diffraction intensities for FC(O)I were recorded with a Gaselectrodiffraction KD-G2^[26] at 25 and 50 cm nozzle-to-plate distances and with an accelerating voltage of ≈60 kV. The sample reservoir was cooled to –50 °C. The inlet system with the nozzle was at room temperature. Two photographic plates of each nozzle-to-plate distance were analyzed with an Agfa DuoscanHiD scanner. Total scattering intensities were derived with the program SCAN3.^[27]

Theoretical force fields for FC(O)I were calculated with the B3LYP method and SDD basis sets. Polarization functions were added for first-row atoms. Vibrational amplitudes and vibrational corrections, $\Delta r = r_a - r_{a^*}$, were derived from these force fields with the program SHRINK.^[28]

IR, Raman, and UV measurements: IR spectra of gaseous samples of FC(O)I were measured in the range 4000–400 cm^{–1} with a Bruker IFS66v spectrometer (Bruker (Germany)) with an optical resolution of 2 cm^{–1}, and 128 scans were co-added for each spectrum.

FT-Raman spectra of a solid sample were measured in the region 3000–50 cm^{–1} on a Bruker RFS100/SFT Raman spectrometer with 1064 nm excitation (500 mW) from a Nd:YAG laser. For this purpose, the sample was condensed as a spot on a nickel-plated copper finger kept at –196 °C in a high vacuum. The solid sample was then excited with the laser through a quartz window. For each spectrum, 256 scans were co-added with a resolution of 4 cm^{–1}.

The gas-phase UV spectrum of FC(O)I was recorded with an Agilent 8453 UV/Vis spectrometer with diode array detection, in the spectral region 190–400 nm. An integration time of 0.5 s and a resolution of 1 nm were used. The sample filled a quartz cell with a 10 cm optical path-length.

NMR measurements: The ¹⁹F, ¹³C, and ¹⁷O NMR spectra of a sample mixed in a 1:1 ratio with CD₂Cl₂ and a trace of CFC₃ as internal standards were recorded at –40 °C on a Bruker Avance300 spectrometer with a ¹⁹F/¹H dual or a multinuclear probe head operating at 282.41, 75.47, or 40.69 MHz, respectively. The 5 mm o.d. sample tube equipped with a rotational symmetrical PTFE valve^[29] was charged at the vacuum line. The $\delta(^{17}\text{O})$ value is referenced against external H₂O.

Mass spectrometry measurements: Mass spectra were recorded with a Finnigan 3300F-100 quadrupole mass spectrometer and the gas samples were introduced by direct injection. A standard ionization energy of 70 eV was used to produce the pattern of fragmentations.

Matrix isolation: The matrix IR spectra were recorded on a Bruker IFS66v FTIR instrument in reflectance mode with a transfer optic. A DTGS detector and a KBr/Ge beam splitter were used in the 5000–400 cm^{–1} region. 64 scans were added for each spectrum with apodized resolutions of 1.2 cm^{–1}. Details of the matrix apparatus have been described elsewhere.^[30] For matrix measurements, small amounts of pure FC(O)I samples (≈0.1 mmol) were transferred in vacuo into a small U-trap kept at –196 °C. This U-trap was mounted in front of the matrix

support and allowed to reach a temperature of –130 °C. A stream of argon gas (1–4 mmol h^{–1}) was directed over the solid FC(O)I, and the resulting gas mixture was immediately quenched on the matrix support at 15 K. A total of 6 matrices with varying amounts (1–5 mmol) and concentrations were prepared and investigated. The photolysis experiments were carried out with a 35 W NNI 40/20 low-pressure mercury lamp (Heraeus Noblelight GmbH, Germany) and a 150 W high-pressure Xe lamp (Amko, Germany) in combination with a water-cooled quartz lens optic, a $\lambda > 320$ nm cut-off, and a 254 nm interference filter (Schott, Germany).

Computational methods: The MOLPRO^[31] program suite was used to calculate the equilibrium structure and harmonic vibrational frequencies of [CO]…[IF] complexes at the coupled-cluster singles and doubles level of theory with a perturbative treatment of connected triple excitations, CCSD(T).^[32,33] Several basis sets were used in this work. For preliminary geometry optimizations, the LanL2DZ basis set augmented with a *d*-polarization function^[34] and a single set of diffuse functions was used for iodine [double zeta (DZ) plus polarization (P) and *s* and *p* diffuse functions (+) and a relativistic effective core potential, DZ+P-REC] together with 6-31+G(d') basis sets for carbon, fluorine, and oxygen atoms (DZ+P). In the final calculations, recently developed diffuse-function-augmented correlation-consistent basis sets for iodine, aug-cc-pVnZ-PP, were used that included a new, small-core (28 electron) relativistic effective core potential (ECP) on iodine.^[35] These ranged in size from [5s4p3d] for the aug-cc-pVDZ-PP to [7s7p4d3f2g] for the aug-cc-pVQZ-PP basis set. Small molecule benchmark calculations^[35] have indicated that any additional errors resulting from the pseudopotential approximation are very small with these ECPs and basis sets. Standard aug-cc-pVnZ (*n* = D, T, Q) basis sets were utilized for carbon, fluorine, and oxygen.^[36,37] In the text and tables, both the aug-cc-pVnZ-PP and aug-cc-pVnZ basis sets will be referred to as simply aug-cc-pVnZ (*n* = D, T, Q).

- [1] *Phosgene and Related Carbonyl Halides*, T. A. Ryan, C. Ryan, E. A. Seddon, K. R. Seddon, Elsevier, Amsterdam, **1996**.
- [2] M. J. Parkington, T. A. Ryan, K. R. Seddon, *J. Chem. Soc. Dalton Trans.* **1997**, 2, 251.
- [3] J. S. Francisco, M. M. Maricq, *Adv. Photochem.* **1995**, 20, 79.
- [4] W. Rüdorff, in *Inorganic Chemistry Part I* (Ed.: W. Klemm), Office of Military Government for Germany, Field Information Agencies Technical (FIAT), Wiesbaden, **1948**, p. 239.
- [5] W. Kwasnik, in *Handbuch der Präparativen Anorganischen Chemie, Vol. 1*, 3rd ed. (Ed.: Georg Brauer), Enke Verlag, Stuttgart, **1975**, p. 225.
- [6] G. Schatte, H. Willner, H. Hoge, E. Knözinger, O. Schrems, *J. Phys. Chem.* **1989**, 93, 6025.
- [7] K. L. D'Amico, M. Trenary, N. D. Shinn, E. I. Solomon, F. R. McFeely, *J. Am. Chem. Soc.* **1982**, 104, 5102.
- [8] D. F. Schriver, P. W. Atkins, *Inorganic Chemistry*, W. H. Freeman, San Francisco, **1990**.
- [9] A. Schriver, L. Schriver-Mazzouli, P. Chaquin, M. Bahou, *J. Phys. Chem. A* **1999**, 103, 2624.
- [10] S. W. Bunte, C. F. Chabalowski, C. Wittig, R. A. Beaudet, *J. Phys. Chem.* **1993**, 97, 5864.
- [11] S. W. Bunte, J. B. Miller, Z. S. Huang, J. E. Verdasco, C. Wittig, R. A. Beaudet, *J. Phys. Chem.* **1992**, 96, 4140.
- [12] L. A. Curtiss, D. J. Pochatko, A. E. Reed, F. Weinhold, *J. Chem. Phys.* **1985**, 82, 2679.
- [13] W. Jäger, Y. Xu, C. L. Gerry, *J. Phys. Chem.* **1993**, 97, 3685.
- [14] J. B. Davey, A. C. Legon, E. R. Waclawik, *Phys. Chem. Chem. Phys.* **1999**, 1, 3097.
- [15] R. M. Romano, A. J. Downs, *J. Phys. Chem. A* **2003**, 107, 5298.
- [16] M. Nakata, K. Kohata, T. Fukuyama, K. Kuchitzu, C. J. Wilkins, *J. Mol. Struct.* **1980**, 68, 271.
- [17] H. Oberhammer, *J. Chem. Phys.* **1980**, 73, 4310.
- [18] P. A. G. Huisman, K. J. Klebe, F. C. Mijlhoff, G. H. Renes, *J. Mol. Struct.* **1979**, 57, 71.
- [19] K. K. Innes, L. E. Giddings, Jr., *J. Mol. Spectrosc.* **1961**, 7, 435.
- [20] I. Zanon, G. Giacometti, D. Picciol, *Spectrochim. Acta* **1963**, 19, 301.

- [21] S. Blanco, A. C. Legon, J. C. Thorn, *J. Chem. Soc. Faraday Trans.* **1994**, *90*, 1365.
- [22] K. Hinds, J. H. Holloway, A. C. Legon, *Chem. Phys. Lett.* **1995**, *242*, 407.
- [23] A. S. Goldman, K. Krogh-Jespersen, *J. Am. Chem. Soc.* **1996**, *118*, 12159.
- [24] C. I. Frum, R. Engleman, Jr., P. F. Bernath, *Chem. Phys. Lett.* **1990**, *167*, 356.
- [25] W. Gombler, H. Willner, *J. Phys. E: Sci. Instrum.* **1987**, *20*, 1286.
- [26] H. Oberhammer, *Molecular Structure by Diffraction Methods, Vol. 4*, The Chemical Society, London, **1976**.
- [27] E. G. Atavin, L. V. Vilkov, *Instrum. Exp. Tech.* **2002**, *45*, 754.
- [28] V. A. Sipachev, *J. Mol. Struct.* **2001**, *67*, 567.
- [29] W. Gombler, H. Willner, *Int. Lab.* **1984**, *14*, 84.
- [30] H. Schnöckel, H. Willner, in *Infrared and Raman Spectroscopy, Methods and Applications* (Ed.: B. Schrader), VCH Weinheim, **1994**, p. 297.
- [31] MOLPRO is a package of ab initio programs written by H. J. Werner and P. J. Knowles with contributions from, J. Almlöf, R. D. Amos, A. Bernhardsson, A. Berning, P. Celani, D. L. Cooper, M. J. O. Deegan, A. J. Dobbyn, F. Eckert, S. T. Elbert, C. Hampel, G. Hetzer, T. Korona, R. Lindh, A. W. Lloyd, S. J. McNicholas, F. R. Manby, W. Meyer, M. E. Mura, A. Nicklass, P. Palmieri, K. A. Peterson, R. M. Pitzer, P. Pulay, G. Runhut, M. Schutz, H. Stoll, A. J. Stone, R. Torroni, P. R. Taylor, T. Thorsteinsson, **2000**.
- [32] C. Hampel, K. A. Petersin, H. J. Wener, *Chem. Phys. Lett.* **1992**, *190*, 1.
- [33] K. Raghavachari, G. W. Trucks, J. A. Pople, M. Head-Gordon, *Chem. Phys. Lett.* **1989**, *157*, 479.
- [34] C. E. Check, T. O. Faust, J. M. Bailey, B. J. Wright, T. M. Gilbert, L. S. Sunderlin, *J. Phys. Chem. A* **2001**, *105*, 8111.
- [35] K. A. Peterson, D. Figgen, E. Goll, H. Stoll, M. Dolg, *J. Chem. Phys.*, submitted.
- [36] T. H. Dunning, Jr., *J. Chem. Phys.* **1980**, *90*, 1007.
- [37] R. A. Kendall, T. H. Dunning, Jr., R. J. Harrison, *J. Chem. Phys.* **1992**, *96*, 6796.

Received: September 3, 2003 [F5506]